502 *Biochemistry* **2011,** *50,* 502–511
DOI: 10.1021/bi101059w

BIOCHEMISTRY
including biophysical chemistry & molecular biology
Article

Direct Measurement of Thermal Stability of Expressed CCR5 and Stabilization by Small Molecule Ligands[†]

Adam M. Knepp, Amy Grunbeck, Sourabh Banerjee, Thomas P. Sakmar, and Thomas Huber*

Laboratory of Molecular Biology and Biochemistry, The Rockefeller University, 1230 York Avenue, New York, New York 10065, United States

Received July 1, 2010; Revised Manuscript Received December 14, 2010

ABSTRACT: The inherent instability of heptahelical G protein-coupled receptors (GPCRs) during purification and reconstitution is a primary impediment to biophysical studies and to obtaining high-resolution crystal structures. New approaches to stabilizing receptors during purification and screening reconstitution procedures are needed. Here we report the development of a novel homogeneous time-resolved fluorescence assay (HTRF) to quantify properly folded CC-chemokine receptor 5 (CCR5). The assay permits high-throughput thermal stability measurements of femtomole quantities of CCR5 in detergent and in engineered nanoscale apolipoprotein-bound bilayer (NABB) particles. We show that recombinantly expressed CCR5 can be incorporated into NABB particles in high yield, resulting in greater thermal stability compared with that of CCR5 in a detergent solution. We also demonstrate that binding of CCR5 to the HIV-1 cellular entry inhibitors maraviroc, AD101, CMPD 167, and vicriviroc dramatically increases receptor stability. The HTRF assay technology reported here is applicable to other membrane proteins and could greatly facilitate structural studies of GPCRs.

G protein-coupled receptors (GPCRs)[1] constitute a large family of heptahelical membrane proteins that recognize a broad array of extracellular ligands and couple to multiple intracellular signaling pathways (*1*, *2*). Their involvement in the molecular pathophysiology of a number of diseases has made GPCRs a major drug target (*3*). Recent high-resolution structures of several GPCRs, including rhodopsin, β_2-adrenergic receptor, β_1-adrenergic receptor, A_{2A} adenosine receptor, and opsin, have provided insight into the molecular mechanism of receptor activation, but further advances are necessary to understand their physiological function and to enhance drug discovery. Stabilizing these complex polytopic membrane proteins in purified and/or defined systems remains the most significant present challenge for biochemists and structural biologists. Successful approaches to generating stable GPCRs in detergent solution include truncations or deletions of disordered regions, insertion of domains such as T4 lysozyme, formation of a complex with an antibody Fab fragment, ligand binding, and introduction of a combination of stabilizing mutations (*4*). These strategies are often difficult or impossible to rationalize, and success with one particular receptor does not guarantee generality.

The study of GPCRs in detergents has limits, even when stabilizing conditions have been identified. Typically, GPCRs, with the possible exception of rhodopsin, are only marginally stable in detergents. Furthermore, the most stabilizing detergents tend to have a low critical micelle concentration (CMC) and relatively large micelle size, which can lead to aggregation phenomena that complicate the interpretation of results (*5*). In general, G protein activity is sharply limited by detergent concentration, making the study of reconstituted ligand−receptor−G protein "signalosomes" in solution impractical (*6*). Nanodisc technology is an attractive alternative to detergents because of its defined lipid bilayer (*7*). We have recently reported the incorporation of rhodopsin, a prototypical GPCR, into discoidal lipoprotein particles called nanoscale apolipoprotein-bound bilayers (NABBs) (*8*). Though incorporation of the β_2-adrenergic receptor and CCR5 into HDL particles has also been recently reported, further functional characterization and optimization of reconstitution conditions are necessary (*9*, *10*). For these reasons, a sensitive, versatile, and high-throughput assay for quantifying properly folded GPCRs and characterizing their stability would have significant utility.

We report here a novel homogeneous time-resolved fluorescence (HTRF) immunosandwich assay based on the simultaneous binding of anti-receptor monoclonal antibodies (mAbs) labeled with a europium cryptate (EuK) fluorescent donor and a modified allophycocyanin (XL665) acceptor. The HTRF technology has previously been applied in monitoring binding of ligand to GPCRs in cell membranes (*11*−*13*). Our HTRF assay enables high-throughput measurements of the thermal stability of recombinantly expressed CCR5 in detergents and NABBs using extremely minute quantities of receptor compared with the

[†]This work was supported by the Tri-Institutional Program in Chemical Biology and National Institutes of Health Grant EY12049.

*To whom correspondence should be addressed: Laboratory of Molecular Biology and Biochemistry, The Rockefeller University, 1230 York Ave., New York, NY 10065. Telephone: (212) 327-8284. Fax: (212) 327-7904. E-mail: hubert@rockefeller.edu.

[1]Abbreviations: GPCR, G protein-coupled receptor; HTRF, homogeneous time-resolved fluorescence; CCR5, CC-chemokine receptor 5; NABB, nanoscale apolipoprotein-bound bilayer; CMC, critical micelle concentration; EuK, europium cryptate; mAb, monoclonal antibody; CHS, cholesteryl hemisuccinate; DOPC, 1,2-dioleoyl-*sn*-glycero-3-phosphocholine; DOPS, 1,2-dioleoyl-*sn*-glycero-3-phospho-L-serine; DM, *n*-dodecyl-β-D-maltoside; CHAPS, 3-[(3-cholamidopropyl)-dimethylammonio]-1-propanesulfonate; LRB, lissamine rhodadmine B; zap1, zebrafish Apo-AI; POPC, 1-palmitoyl-2-oleoyl-*sn*-glycero-3-phosphocholine; DOPE, 1,2-dioleoyl-*sn*-glycero-3-phosphoethanolamine; SPR, surface plasmon resonance.

 Published on Web 12/14/2010

amount used in existing approaches (*14*, *15*). We show that CCR5 NABBs are more stable than the detergent-solubilized receptor, suggesting that NABBs are a viable platform for biochemical and biophysical study. We also studied the effects of the small molecule antagonists maraviroc, AD101, CMPD 167, and vicriviroc on CCR5 thermal stability. Using the HTRF assay, we found that the antagonists inhibit binding of 2D7 mAb to its conformationally sensitive epitope on the EC2 loop to varying degrees, but none completely. Further, the melting curves demonstrate that the small molecules confer a striking increase in CCR5 thermal stability. This suggests that these high-affinity ligands trap the receptor in a single conformation and prevent denaturation. The antagonist−CCR5 complexes should be promising candidates for structural studies.

MATERIALS AND METHODS

Cells, Plasmids, and Reagents. HEK-293T cells were obtained from the American Type Culture Collection (Manassas, VA). Transfection reagents were obtained from Invitrogen (Carlsbad, CA). Lipids were obtained from Avanti Polar Lipids (Alabaster, AL), except cholesterol, which was obtained from Sigma-Aldrich (St. Louis, MO). Detergents were obtained from Anatrace, Inc. (Maumee, OH). HTRF reagents were obtained from Cisbio (Bedford, MA). All time-resolved FRET assays were performed on a PerkinElmer EnVision Multilabel Plate Reader. Buffer N consisted of 20 mM Tris-HCl (pH 7.0), 0.1 M $(NH_4)_2SO_4$, 10% (v/v) glycerol, 0.07% cholesteryl hemisuccinate (CHS), 0.018% 1,2-dioleoyl-*sn*-glycero-3-phosphocholine (DOPC), 0.008% 1,2-dioleoyl-*sn*-glycero-3-phospho-L-serine (DOPS), 0.33% *n*-dodecyl β-D-maltoside (DM), and 0.33% 3-[(3-cholamidopropyl)-dimethylammonio]-1-propanesulfonate (CHAPS). Buffer E1 consisted of buffer N supplemented with 400 μM 1D5-nonapeptide corresponding to the engineered C-terminal receptor epitope. Buffer S consisted of 20 mM Tris-HCl (pH 7.0), 100 mM $(NH_4)_2SO_4$, and 10% (v/v) glycerol. Buffer C consisted of 100 mM phosphate and 150 mM NaCl (pH 7.2). Buffer P consisted of 100 mM phosphate and 150 mM NaCl (pH 7.5). Buffer E2 consisted of buffer P supplemented with 200 mM imidazole. Buffer G consisted of 100 mM phosphate, 150 mM NaCl, and 0.5 mg/mL BSA (pH 7.0).

Preparation of Lipids. Lipids were dissolved in chloroform at a concentration of approximately 100 mg/mL in glass round-bottom flasks. The solvent was evaporated under a gentle stream of dry argon while the flask was rotated, forming a thin lipid film. The lipids were redissolved in dichloromethane, and the procedure was repeated. The remaining dichloromethane was removed under vacuum overnight. The lipid films were then hydrated with the appropriate detergent-containing buffers, sonicated, and frozen and thawed in liquid N_2 until they were fully solubilized.

Transient Transfection of HEK Cells and Solubilization of Heterologously Expressed CCR5. HEK-293T cells were grown in Dulbecco's modified Eagle's medium (DMEM) [4.5 g/L glucose and 2 mM glutamine (Gibco)] supplemented with 10% fetal bovine serum (FBS) (Atlanta Biologicals) at 37 °C in a 5% CO_2 atmosphere. HEK-293T cells were transfected with human CCR5 cDNA tagged with the C-terminal 1D4 epitope, TETSQVAPA, in pcDNA3.1(+) using Lipofectamine Plus as previously described for earlier experiments with rhodopsin (*16*). Briefly, for one 10 cm plate, 0.75 mL of prewarmed DMEM was mixed with 3.5 μg of plasmid DNA. To this was added 10 μL of PLUS reagent, and the mixture was incubated for 15 min and then transferred to a separate mixture containing 0.5 mL of DMEM and 17 μL of Lipofectamine Plus. After another 15 min incubation, the volume was increased to 4 mL with DMEM and the mixture added to HEK-293T cells at 70−80% confluence. Four hours after transfection, an additional 4 mL of DMEM supplemented with 20% FBS was added. Cells expressing CCR5 were harvested 48 h after transfection in PBS buffer containing the protease inhibitors aprotinin and leupeptin. Cell pellets from 10 cm plates were lysed in 1 mL of buffer N (supplemented with protease inhibitors) per 5×10^6 cells. After thorough resuspension, the solution was probe-tip sonicated with 6×1 s pulses and incubated for 2 h at 4 °C. The solution was then centrifuged at 20000*g* for 20 min at 4 °C. The supernatant fraction was collected and stored at −80 °C until further use.

Immobilization of the 1D4 Monoclonal Antibody. Anti-rhodopsin antibody 1D4 was immobilized on cyanogen bromide-activated Sepharose 2B (Sigma-Aldrich), a bead-formed agarose-based gel filtration matrix with 2% agarose content, using established protocols with slight modifications (*17*, *18*). In a fume hood, 30 mL of packed Sepharose 2B in a total volume of 60 mL of 2 M sodium carbonate buffer (pH 11) was treated with 3 g of CNBr in 3 mL of acetonitrile on an ice bath under gentle agitation with a suspended magnetic stirrer. The pH of the reaction mixture was kept at 10−11 by titration with 1 N NaOH over a period of 30 min. The activated beads were washed under suction four times with 50 mL of ice-cold water and twice with 50 mL of cold coupling buffer [150 mM sodium chloride and 10 mM sodium borate buffer (pH 8.2)]. Twenty-five milliliters of packed beads was immediately incubated with 50 mg of 1D4 mAb in a total volume of coupling buffer of 50 mL with head-over-head mixing at 4 °C overnight. Finally, the matrix was washed at 4 °C with 100 mL aliquots of phosphate-buffered saline (pH 7.4), once with 10 mM glycine for 20 min and four times without glycine. The matrix was stored in the presence of 0.065% sodium azide. The protein binding was quantitative with 2 mg of antibody/mL of settled beads, and the resulting binding capacity for rhodopsin was 0.4 mg/mL, as determined spectrophotometrically using solubilized rod outer segment disk membranes (*8*).

Purification of Heterologously Expressed CCR5 and Incorporation into NABBs. Solubilized lysate from $2 \times$ 10 cm plates was thawed on ice and added to 50 μL of packed beads of 1D4-Sepharose resin with 2 mg/mL immobilized 1D4 mAb. The lysate/resin mixture was incubated for 16 h at 4 °C. The resin was transferred to a Micro-Spin column (Pierce), centrifuged to remove the supernatant fraction, and washed twice with buffer N. Purified CCR5 was eluted by incubating the resin with 2×50 μL of buffer E1 for 30 min. The NABB mixture was made via addition of the combined CCR5 elutions to 3.75 nmol of purified zap1 prepared as described previously (*8*), 280 nmol of 1-palmitoyl-2-oleoyl-*sn*-glycero-3-phosphocholine (POPC), and 22.7 nmol of cholesterol in a total volume of 200 μL containing 1.5% sodium cholate, 0.33% DM, 15 mM Tris-HCl (pH 7.0), 75 mM $(NH_4)_2SO_4$, and 7.5% glycerol. When desired, a POPC solution containing 0.5% lissamine rhodadmine B-labeled 1,2-dioleoyl-*sn*-glycero-3-phosphoethanolamine (LRB-DOPE) was used to allow visualization of NABB elution. After being vortexed and incubated on ice for 30 min, the mixture was added to 1 mL of Pierce Detergent Removal Resin pre-equilibrated with at least 1 column volume of buffer S. Elution was conducted at 4 °C under gravity flow by addition of buffer S to the column and collection of 200 μL fractions. Fractions were analyzed for protein content by monitoring the absorbance at 280 nm. Protein-containing fractions were pooled and applied to a

Superose 6 10/300 gel filtration column. Absorbance at 280 nm (protein) and, when applicable, 570 nm (LRB-DOPE) was monitored with an in-line detector in the FPLC instrument (Akta Explorer, GE). Fractions of the peak corresponding to NABBs were combined and, if necessary, concentrated using an Amicon Ultra 30 kDa cutoff centrifugal filter device (Millipore). For the 2D7 immunoprecipitation experiment, CCR5 NABBs were mixed with Dynabeads Protein G (Invitrogen) with or without 2D7 mAb (BD Biosciences) according to the manufacturer's protocol. After overnight incubation at 4 °C, the supernatant fractions were subjected to 1D4 immunoblot analysis as described below.

Immunoblot Analysis. Samples were resolved by sodium dodecyl sulfate−polyacrylamide gel electrophoresis (SDS−PAGE) (NuPage Novex 4−12% Bis-Tris Gel) and transferred onto Immobilon, a polyvinylidene difluoride (PVDF) membrane (Millipore), according to the manufacturer's protocol. For CCR5 detection, membranes were probed with primary antibodies against the engineered 1D4 epitope (National Cell Culture Center; 1:5000) followed by a horseradish peroxidase (HRP)-conjugated anti-mouse secondary antibody (Amersham Biosciences GE; 1:10000). For zap1 detection, an α-His_6 tag monoclonal antibody was used (Sigma; 1:5000) followed by HRP-α-mouse. Signals were visualized by enhanced chemiluminescence treatment (Amersham Biosciences GE) and exposed to HyBlot CL autoradiography film (Denville Scientific, Inc.).

Fluorescein-Maraviroc Binding to Solubilized CCR5. Solubilized CCR5 lysate from approximately one-fifth of a plate was incubated with 100 nM fluorescein-labeled maraviroc analogue (FL-maraviroc; generously provided by M. Teintze, Montana State University, Bozeman, MT) and 12.5 μL of 1D4-Sepharose resin (2 mg of 1D4 mAb/mL of packed resin) for 16 h at 4 °C in the presence and absence of 1 μM unlabeled maraviroc (Toronto Research Chemicals). The beads were washed three times with buffer N, and samples were eluted via incubation of the beads with 1% SDS for 1 h at room temperature and shaking. Eluted samples were transferred to a black 96-well round-bottom polypropylene microtiter plate (Nunc/Thermo Fisher Scientific). A serial dilution of FL-maraviroc in 1% SDS was also included for a standard curve. The plate was read on a Cytofluor II Fluorescence Multiwell Plate Reader (Perbio Science) with an excitation wavelength of 485 nm and an emission wavelength of 530 nm. A linear fit of the standard curve was used to calculate the concentration of FL-maraviroc bound to the CCR5 lysate. The difference between the values with and without excess unlabeled maraviroc was used to calculate the CCR5 concentration with a correction for nonspecific binding of FL-maraviroc.

Biotinylation of IgG. A 20 mM sodium *m*-periodate solution was made in 100 mM sodium acetate (pH 5.5) and mixed with an equal volume of 2 mg/mL 1D4 mAb in buffer C. The mixture was covered in aluminum foil to protect it from light and incubated for 30 min at 4 °C. The mixture was then dialyzed against buffer C for 4 h to remove excess periodate. Biocytin-hydrazide (Pierce) was prepared as a 50 mM stock in DMSO and diluted to a final concentration of 2.9 mM in the 1D4 solution. The coupling reaction was allowed to proceed for 3.5 h at room temperature, and unreacted material was removed by dialysis against buffer C. To improve the stability of the conjugate, 1D4-biotin was reduced with sodium cyanoborohydride in the following manner. A 5 M stock of $NaBH_3(CN)$ was prepared in 1 M KOH. To 200 μL of 1D4-biotin were added 1 mL of buffer C and 12 μL of 5 M $NaBH_3(CN)$. The reaction proceeded overnight at 4 °C while the mixture was protected from light, and the mixture was then dialyzed against buffer C. The biotin:1D4 ratio was determined to be 0.7 using the Pierce biotin quantitation kit according to the manufacturer's protocol. 1D4-biotin was stored at 4 °C with 0.02% NaN_3.

Solid-Phase Labeling of IgG with Europium Cryptate. Ni-NTA magnetic agarose beads (QIAGEN; 200 μL, 5% slurry) were washed with 1 mL of buffer P. 2D7 mAb (100 μg, 1.3 nmol) was bound to beads via incubation for 30 min at room temperature with shaking. In all solid-phase reactions, 0.0037% (w/v) DM was added to facilitate mixing. The beads were spun down, and the tube was placed on a magnetic rack to ease removal of the supernatant fraction. The antibody was activated via addition of 2 μL of 3.75 mM sulfo-SMCC (Pierce; 7.5 nmol, 5.6 equiv) and shaking for 60 min at room temperature. In a separate reaction, 3.68 μL of 0.68 mM europium trisbipyridine diamino cryptate (EuK) (Cisbio; 2.5 nmol), 0.67 μL of 0.5 M sodium borate (pH 8.2), 1.32 μL of 1 M NaF, and 0.67 μL of 7.58 mM SPDP (Pierce; 5.0 nmol, 2 equiv) were mixed for 60 min at room temperature with shaking. The EuK−SPDP reaction was stopped by addition of 0.67 μL of 7.58 mM Tris. SPDP was reduced via addition of 0.67 μL of 8.27 mM TCEP and mixing for 15 min. The activated EuK was added to activated IgG and mixed overnight at 4 °C. The conjugation reaction was stopped with 1 μL of 80 mM *N*-acetylcysteine. The beads were washed twice with 1 mL of buffer P. IgG was eluted with two 50 μL volumes of buffer E2 for 30 min each. Combined elutions were supplemented with 0.5 mg/mL bovine serum albumin (BSA) and run on a Superdex 200 10/300 GL gel filtration column in buffer G. Absorbance was monitored at 280 and 305 nm for protein and EuK content, respectively. 2D7-EuK was stored at 4 °C with 0.01% thiomersal.

HTRF Assay for Quantifying Folded CCR5. All HTRF assays were conducted with the appropriate buffer supplemented with 50 mM NaF and 1 mg/mL BSA. Biotinylated 1D4 mAb was mixed with streptavidin-XL665 (SA-XL665) (Cisbio) for 15 min on ice at a final concentration of 128 nM. To this was added an equal volume of 8 nM EuK-labeled 2D7 mAb (2D7-EuK). For each well of the experiment, 20 μL of this mixture was added to a black bottom 384-well microplate (Greiner). Solubilized CCR5 or CCR5 in NABBs was added to a final volume of 40 μL. The final concentrations of labeled assay components were as follows: 32 nM 1D4-biotin, 32 nM SA-XL665, and 2 nM 2D7-EuK. In competition experiments, CCR5 was preincubated with competitors for 30 min on ice prior to addition to fluorescently labeled components in the 384-well plate. To obtain the maximal signal, we incubated the plate overnight at 4 °C. Dual-channel fluorescence was measured with excitation at 320 nm and emission collection in ten 200 μs windows at 615 and 665 nm. An acceptable signal-to-background ratio was achieved with 5000 flashes per well. Emission counts were summed over all windows except the first, and the F_{665}/F_{615} ratio was used as a normalized measure of sensitized emission. As an assay-to-assay control, signal enhancement ΔF was calculated:

$$\Delta F = \left(\frac{F_{665,\,\mathrm{sample}}}{F_{615,\,\mathrm{sample}}} - \frac{F_{665,\,\mathrm{negative}}}{F_{615,\,\mathrm{negative}}}\right) \Big/ \frac{F_{665,\,\mathrm{negative}}}{F_{615,\,\mathrm{negative}}} \qquad (1)$$

where the negative control values are obtained from the mixed labeled components in the absence of receptor.

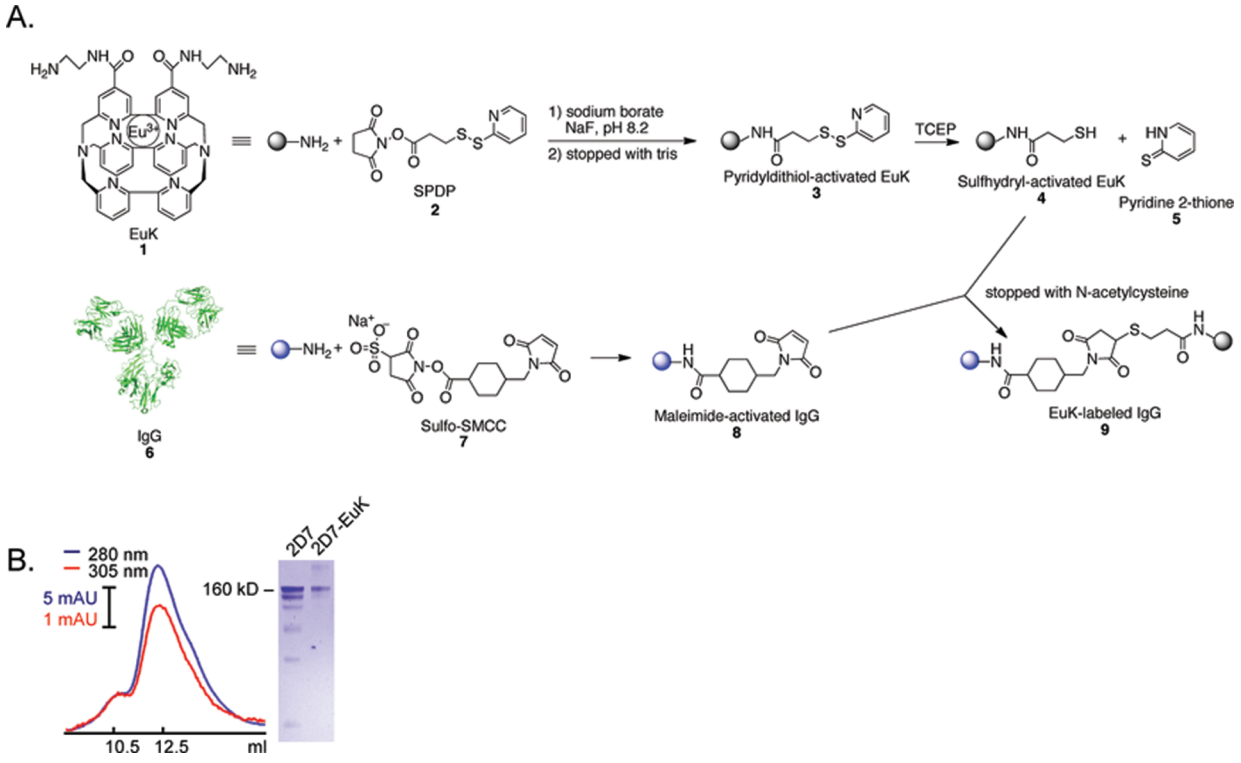

FIGURE 1: (A) Scheme depicting the strategy for synthesizing EuK-labeled 2D7 mAb (**9**). EuK (**1**) is activated by addition of a sulfhydryl by reaction with SPDP (**2**) and reduction by TCEP (top). Separately, 2D7 mAb (**6**) is immobilized on Ni-NTA resin and reacted with sulfo-SMCC (**7**) to generate a maleimide derivative (**8**). A crystal structure of IgG [Protein Data Bank (PDB) entry 1IGY] is shown as a model. The two activated reagents are combined, and labeled 2D7 is eluted from the resin with imidazole. (B) Size-exclusion chromatography with monitoring of absorbance at 280 nm (blue, protein) and 305 nm (red, EuK) to determine the yield and labeling ratio (left). Coomassie blue-stained nonreducing SDS−polyacrylamide gel electrophoresis showing a single band of the intact 2D7-EuK after labeling (right). Note the impurities of the initial 2D7 sample have been largely removed by the procedure.

CCR5 Thermal Stability Measurements Using HTRF. Detergent-solubilized CCR5 or CCR5 NABBs were diluted to a concentration within the dynamic range of the HTRF assay, and 11 μL aliquots were added to polymerase chain reaction (PCR) tubes. For experiments testing the stabilizing effects of the small molecule antagonists maraviroc, AD101, CMPD 167, and vicriviroc, the receptor was preincubated with 8 μM ligand for 1 h on ice before the next step. The CCR5-containing tubes were transferred to a Multigene Gradient Thermal Cycler (Labnet International, Inc.). The thermal cycler was set up to apply a gradient of temperatures across a row of the heating block for 30 min, followed by cooling to 4 °C. Each sample was diluted by a factor of 2 in the appropriate buffer, and 20 μL of the heat-treated material was added to each well of a 384-well microplate containing 20 μL of the fluorescently labeled components.

Modeling Thermal Denaturation of CCR5 and CCR5−Ligand Complexes. Denaturation of unliganded CCR5 in detergent solution and NABBs was modeled as a simple first-order process.

$$[\text{unliganded, folded}] \xrightarrow{k} [\text{unfolded}] \tag{2}$$

The HTRF signal ΔF is the sum of contributions from folded and unfolded receptor with appropriate scaling factors.

$$\Delta F = \alpha_1[\text{unliganded, folded}] + \alpha_2[\text{unfolded}] \tag{3}$$

Because denatured receptor does not bind 2D7-EuK, α_2 was set to zero. The signal is then

$$\Delta F = \alpha_1 e^{-kt} \tag{4}$$

with

$$k = Ae^{-E_a/RT} \tag{5}$$

The curve was fit with parameters α_1, A, and E_a; T_M was defined as the temperature at which one-half of the receptor is unfolded. The time of incubation is designated as t. The temperature of incubation, T, was specified in kelvin.

Melting of CCR5−ligand complexes was modeled similarly, but as a two-step sequence with a first-order reaction describing the irreversible conversion of the "loose" and "tight" binding states and a second irreversible denaturation step from the tight state. This model assumes that no unliganded receptor exists in the system, which is likely to be true because of the high affinity of the antagonists tested.

$$[\text{liganded, loose, folded}] \xrightarrow{k_1} [\text{liganded, tight, folded}] \xrightarrow{k_2} [\text{unfolded}] \tag{6}$$

The HTRF signal in this system is the sum of contributions from these three species.

$$\Delta F = \alpha_1[\text{liganded, loose, folded}] + \alpha_2[\text{liganded, tight, folded}] + \alpha_3[\text{unfolded}] \tag{7}$$

Again, the scaling factor for unfolded receptor, α_3, was set to zero, making the total signal

$$\Delta F = \alpha_1 e^{-k_1 t} + \alpha_2 \left[\frac{k_1}{k_2 - k_1}(e^{-k_1 t} - e^{-k_2 t})\right]$$

with

$$k_1 = A_1 e^{-E_{a,1}/RT} \quad (8)$$

$$k_2 = A_2 e^{-E_{a,2}/RT} \quad (9)$$

The curve was fit with parameters α_1, A_1, $E_{a,1}$, α_2, A_2, and $E_{a,2}$; T_M was defined as the temperature at which one-half of the receptor is unfolded. It is important to note that these models assume that the conversion from the loosely to the tightly bound state and the denaturation are irreversible processes. Moreover, we restrict our interpretation of the model to a single derived parameter, the apparent melting temperature, T_M.

RESULTS

Solid-Phase Labeling of IgG with EuK. We first developed a solid-phase strategy to label directly 2D7 mAb with EuK. Magnetic Ni-NTA beads were used to immobilize 2D7 by binding to a histidine-rich region of the Fc stem, permitting efficient wash and elution steps. 2D7-EuK was then prepared in a three-step reaction scheme (Figure 1A). We found that activating 2D7 with SPDP, as previously reported, resulted in significant reduction of IgG disulfide linkages after addition of TCEP (data not shown) (*19*, *20*). To avoid this problem, we inverted the activation steps, reacting 2D7 with sulfo-SMCC and EuK with SPDP. The reduction step was thus conducted in the absence of antibody, resulting in minimal antibody fragmentation as shown by comparing labeled 2D7 to starting material on a Coomassie Blue-stained SDS−PAGE gel (Figure 1B, right).

After labeled 2D7 had been eluted from the magnetic beads, the sample was purified by gel filtration chromatography (Figure 1B, left). Absorbance was monitored at 280 nm (protein) and 305 nm (EuK). Using the integrated absorbance peaks and known molar extinction coefficients (*21*), the labeling ratio was estimated to be 1.3 EuK/IgG. The main peak in the chromatogram is monomeric 2D7-EuK. Dimeric 2D7 elutes slightly earlier, and the right shoulder of the peak is likely to represent small quantities of antibody fragments. EuK fluorescence at 615 nm was measured for each column fraction (data not shown); the profile was fit to three Gaussian peaks, and fractions determined most likely to contain monomer were pooled. The recovery of 2D7-EuK was >30 μg from the 100 μg of 2D7 starting material, with monomeric IgG constituting an estimated 90% of the protein content. Including bovine serum albumin (BSA) as a carrier protein during the size exclusion chromatography purification step contributed significantly to the high yield of the labeled antibody.

Characterization of the HTRF Assay with Solubilized CCR5. CCR5 was heterologously expressed in transiently transfected HEK-293T cells and solubilized in a detergent-containing buffer previously shown to preserve proper CCR5 folding (*22*). We estimated the total receptor concentration by incubating CCR5 with a saturating amount of a fluorescein-derivatized maraviroc analogue (FL-maraviroc). CCR5 was immunoprecipitated on 1D4-Sepharose beads, and the amount of receptor was calculated by comparing the fluorescent signal in the elution to a FL-maraviroc standard curve (Figure S1 of the Supporting Information). Using this method, the concentration of CCR5 in cell lysate was estimated to be 13.9 ± 0.2 nM. This concentration represents a lower bound, though we assume that all folded receptor can bind the high-affinity ligand.

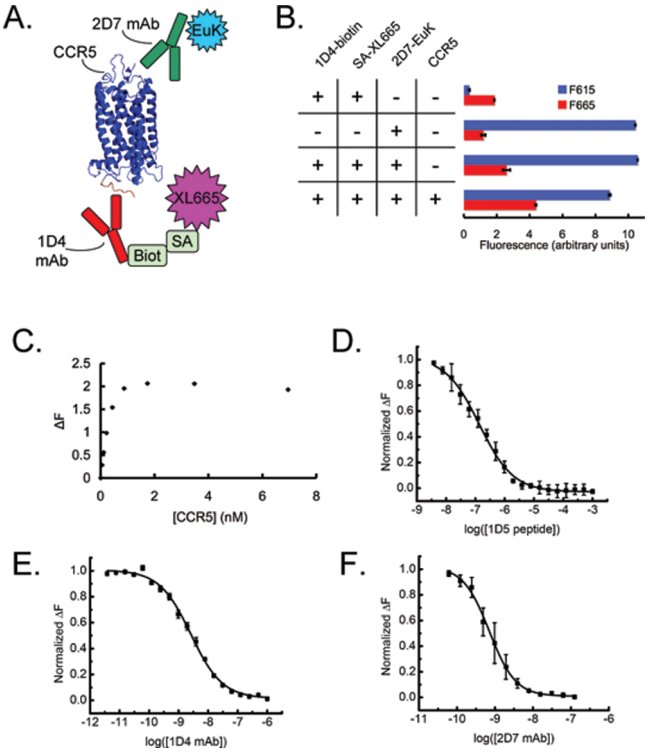

FIGURE 2: (A) HTRF sandwich immunoassay schematic. A hypothetical model of CCR5 based on the crystal structure of rhodopsin (PDB entry 1U19) is shown. 2D7-EuK recognizes a conformation-sensitive split epitope on the extracellular side of CCR5. Biotinylated 1D4 (1D4-biot) binds an engineered nine-residue C-terminal epitope (red) and is linked to streptavidin-conjugated XL665. FRET is observed between EuK and XL665 when 2D7 binds properly folded CCR5. The Förster radius for this donor−acceptor pair is approximately 95 Å. (B) Assay controls with fluorescence counts at 615 nm (blue) and 665 nm (red) after excitation at 320 nm. The CCR5-specific signal is seen as an increase at 665 nm and a decrease at 615 nm. (C) Serial dilution of CCR5 showing the dynamic range of the assay. The signal is saturated at ~200% enhancement over background. ΔF is defined as $(F_{665,sample}/F_{615,sample} - F_{665,negative}/F_{615,negative})/F_{665,negative}/F_{665,negative}$. (D−F) Competition experiments with the 1D5 nonapeptide (D), 1D4 mAb (E), and 2D7 mAb (F) demonstrate signal specificity. The apparent IC_{50} values are 130, 2.7, and 0.79 nM for the three competitors, respectively.

The HTRF assay relies on simultaneous binding of 2D7-EuK and 1D4-biotin to CCR5, and 1D4-biotin binding to SA-XL665 (Figure 2A). Preliminary optimization experiments demonstrated that the maximal signal was achieved with an excess of 1D4-biotin and SA-XL665 compared to 2D7-EuK. For signal reproducibility, the assay mixtures were incubated overnight at 4 °C before fluorescence was read. The assay was characterized using negative controls without the labeled antibodies (Figure 2B). 1D4-biotin/SA-XL665 in the absence of a fluorescent donor results in minimal counts at 615 nm and some emission at 665 nm. 2D7-EuK in the absence of the acceptor complex gives a strong signal at 615 nm and less emission at 665 nm than XL665. The standard negative control was a mixture of 1D4-biotin, SA-XL665, and 2D7-EuK. Under these conditions, the 615 nm signal was roughly the same as 2D7-EuK alone, and the 665 nm signal was only slightly stronger than that from 1D4-biotin/SA-XL665 only. This result suggests minimal sensitized emission of XL665 in the absence of CCR5. The CCR5-specific signal manifests as a decrease in 615 nm fluorescence and an increase in 665 nm fluorescence as the FRET donor and acceptor are brought into proximity by binding receptor.

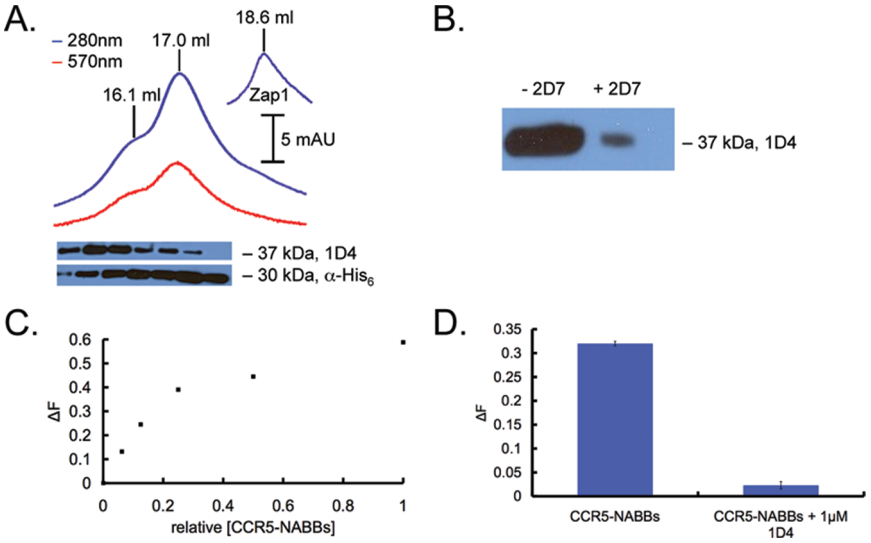

FIGURE 3: (A) Chromatogram showing coelution of the protein (blue, 280 nm) and fluorescent lipids (red, 570 nm). The 1D4 immunoblot below shows that CCR5 NABBs elute in the peak centered at 15.6 mL, exhibiting a larger hydrodynamic radius than the majority of the NABBs at 16.1 and 17.0 mL. The anti-His_6 blot detects His-tagged zap1 belt protein. Free zap1 elutes at 18.6 mL (inset). (B) CCR5 NABBs were incubated with Protein G beads and 2D7, and the supernatant fraction was probed with a 1D4 immunoblot. The majority of CCR5 in NABBs is immunoprecipitated by 2D7, indicating the properly folded receptor. (C) HTRF signal from a serial dilution of CCR5 NABBs, demonstrating the ability to quantify properly folded CCR5 in NABBs. (D) The HTRF signal is efficiently competed with 1 μM 1D4, showing signal specificity.

Measurements with a serial dilution of the solubilized lysate containing CCR5 revealed the dynamic range of the assay (Figure 2C). A characteristic linear range precedes signal saturation near 200% over background at high concentrations. The measurement errors are approximately 2% of the background signal as determined by standard error propagation. Using the FL-maraviroc binding experiment for calibration, an estimated 0.02−1.0 nM CCR5 can be effectively quantified. In a volume of 40 μL, this corresponds to 0.8−40 fmol of receptor. Signal saturation near 2 nM, the concentration of 2D7-EuK, suggests that this antibody has a high affinity compared to the concentrations involved. In subsequent experiments, receptor concentrations near the middle of the dynamic range were used to minimize measurement errors.

The specificity of the HTRF signal for CCR5 epitopes was demonstrated in competition experiments. CCR5 was preincubated with a serial dilution of TETSQVAPA nonapeptide ("1D5"), 1D4, and 2D7 (Figure 2D−F). 1D5-nonapeptide corresponds to the engineered C-terminal epitope on the receptor. These competition data were fit to a sigmoidal curve. Signal enhancement ΔF was normalized to the end points at 0% inhibition and 100% inhibition. The calculated IC_{50} values for 1D5, 1D4, and 2D7 were 130, 2.7, and 0.79 nM, respectively. The IC_{50} values of 1D4 and 2D7 are lower than the concentrations of 1D4-biotin and 2D7-EuK in the assay, suggesting that the labeled antibodies may have slightly reduced binding capacity and/or affinity. Having shown the specificity of the signal, we next focused on applying the assay technology to the problem of CCR5 reconstitution.

Optimizing Microincorporation of CCR5 into NABBs using HTRF. We have previously reported the incorporation of rod outer segment bovine rhodopsin into NABB particles (*8*). Unlike rhodopsin, CCR5 cannot be purified in large quantities from natural sources, so we employed a microscale approach to optimize a procedure to reconstitute functionally expressed CCR5 in NABBs. The general procedure is outlined in Figure S2 of the Supporting Information. Recombinantly expressed CCR5 was immunopurified from the solubilized lysate using 1D4-Sepharose beads. After several washing steps, receptor was eluted by addition of 1D5-nonapeptide. Roughly one-half of the receptor is lost in this purification step because of incomplete elution from the beads. [Elution is also the theoretical limiting step in rhodopsin purification using 1D4-Sepharose beads (T. P. Sakmar, unpublished observation)] The NABB assembly mixture was formed by mixing purified zebrafish Apo-A1 (zap1) and lipids at a molar ratio of 1:75, which we showed yields 10−12 nm diameter disks in our earlier rhodopsin NABB study (*8*). Purified CCR5 elution was added to this mixture and, after incubation on ice, applied to a detergent-removal resin. NABBs were eluted under gravity flow by addition of detergent-free buffer, and fractions were collected. Protein-containing fractions were determined by measurement of 280 nm absorbance and pooled.

The combined elutions were run on a gel filtration column for characterization and purification (Figure 3A). Co-elution of protein and lipids was monitored by measuring absorption at 280 and 570 nm, which detected rhodamine-DOPE-labeled POPC. Immunoblots showed the relative content of CCR5 (1D4 mAb detection) and zap1 (α-His_6 mAb detection) in each fraction. The majority of the CCR5 NABBs elute at 15.6 mL in the shoulder of the first peak, which is centered at ~16.1 mL. The second peak, at ~17 mL, contains mainly empty NABBs. In our previous study of rhodopsin NABBs reconstituted at a similar ratio, we also observed that the receptor-containing NABBs elute ~0.5 mL earlier than the majority of empty NABBs. Note that the ratio of CCR5 to NABBs is approximately 1:100. This strategy reduces the likelihood of incorporating more than one receptor per NABB and guarantees a relatively homogeneous CCR5 NABB preparation. Free zap1, which elutes at ~18.6 mL (Figure 3A, inset), likely constitutes the right peak shoulder that is rather lipid-poor as judged by the 570 nm absorbance. The CCR5 NABBs were mixed with Protein G beads with (left) and without (right) 2D7, and the supernatant fractions were subjected to 1D4 immunoblot analysis (Figure 3B). The near-quantitative immunoprecipitation of CCR5 NABBs with the conformationally sensitive 2D7 antibody suggests that most of the receptor is properly folded.

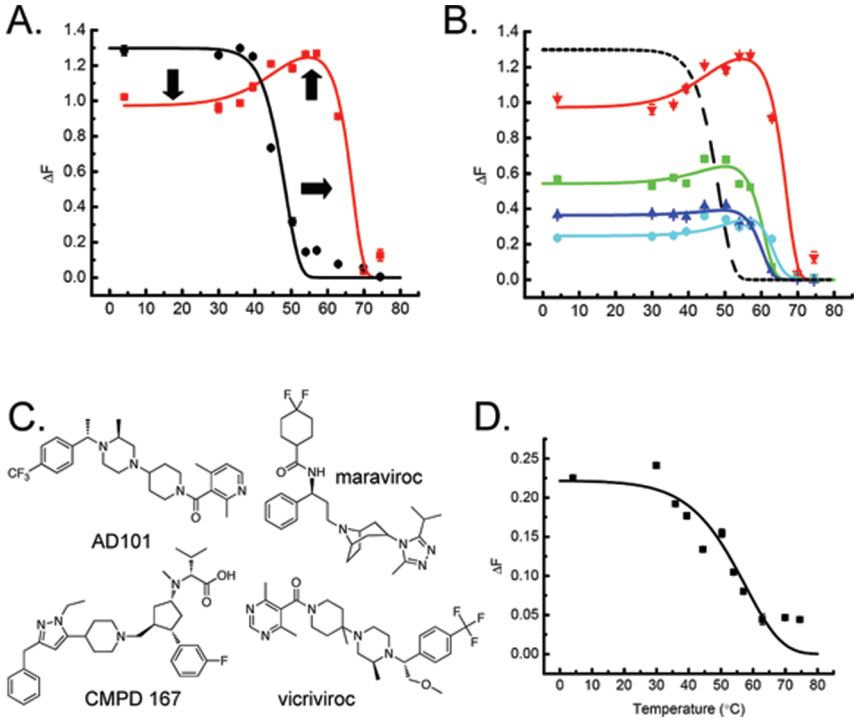

FIGURE 4: HTRF assay applied to take high-throughput thermal stability measurements with femtomole quantities of CCR5. A range of temperatures was used for detergent-solubilized CCR5 or CCR5 NABBs before the addition of labeled HTRF components in a 384-well plate. (A) Melting curves of unliganded CCR5 (black) and CCR5 preincubated with the small molecule antagonist maraviroc (red). Maraviroc shifts the T_M of detergent-solubilized CCR5 from 47.1 to 66.0 °C (rightward-pointing arrow) and appears to display a two-step binding profile. The first ligand−receptor state reduces the accessibility of the 2D7 epitope on the EC2 loop compared with that of the unliganded receptor (downward-pointing arrow). The second ligand−receptor state results in a stronger HTRF signal (upward-pointing arrow). (B) Thermal denaturation of CCR5−ligand complexes. CCR5 was preincubated with maraviroc (red), AD101 (green), vicriviroc (blue), and CMPD 167 (cyan). All of these antagonists appear to have two binding states. The calculated T_M values for maraviroc, AD101, vicriviroc, and CMPD 167 are 66.0, 59.9, 59.5, and 62.7 °C, respectively. The unliganded receptor, which melts at a lower temperature, is shown as a black dashed line for reference. (C) Molecular structures of the CCR5 antagonists tested. (D) Melting curve of CCR5 NABBs. The assembly denatures at 54.5 °C. CCR5 NABBs melt over a much broader range than CCR5 in detergent solution, suggesting some sample heterogeneity or a distinct denaturation pathway.

The HTRF assay was used in conjunction with gel filtration chromatography and immunoblot analysis to facilitate optimization of preparation conditions. The HTRF assay complements immunoblots because it reports on receptor folding, not just the total amount of receptor protein. Moreover, the HTRF assay is much more quantitative and reproducible. 2D7-EuK and 1D4-biotin bind to CCR5 in NABBs, resulting in a dynamic range for the HTRF assay as with the detergent-solubilized receptor (Figure 3C). Competition with 1 μM 1D4 ablates the signal, demonstrating signal specificity as in detergent solution (Figure 3D). Assay conditions were identical to those in detergent experiments, except that phosphate-buffered saline (PBS) was used as the starting buffer.

Using the HTRF signal as a guide, we screened a number of conditions for optimal formation of CCR5 NABBs containing correctly folded receptor. Variables included changing the detergents used, the zap1:lipid ratio, the lipid composition, and the detergent-removal resin elution buffer. We found that several factors were particularly important for optimal CCR5 recovery. Elution of CCR5 from 1D4-Sepharose beads in buffer N and inclusion of 0.3% (w/v) *n*-dodecyl β-D-maltopyranoside (DM) in the final NABB mixture enhanced stability. Notably, the detergent removal resin adequately extracted DM despite its low CMC. Including cholesterol at a cholesterol:POPC molar ratio of 7.5:92.5 also improved CCR5 incorporation. Finally, equilibrating and eluting from the detergent removal resin with buffer S, 20 mM Tris-HCl (pH 7.0), 0.1 M $(NH_4)_2SO_4$, and 10% (v/v) glycerol further increased recovery. Comparing the HTRF signal from CCR5 NABBs to that of the solubilized CCR5 starting material, the overall yield of correctly folded receptor in the optimized procedure was >15%. This estimate likely represents a lower bound because the NABB might prevent head-to-tail donor−acceptor interactions that theoretically may cause a reduction in the donor−acceptor distance and an increase in HTRF signal intensity in detergent. Indeed, it appears that the HTRF signal at a saturating concentration of CCR5 NABBs is weaker than the maximal signal in detergent solution (Figures 2C and 3C).

High-Throughput Thermal Stability Measurements of CCR5. Thermal stability is a crucial indicator of receptor tractability outside of its native membrane environment. We adapted the HTRF assay to measure CCR5 thermal stability under a variety of conditions. In short, a range of temperatures was applied to CCR5 aliquots for 30 min, and then the samples were cooled to 4 °C and added to the microplate containing the labeled 1D4 and 2D7 FRET pair. Plotting the ratio of the fluorescence signal as a function of temperature generates thermal denaturation or melting curves (Figure 4). Receptor denaturation and subsequent loss of 2D7-EuK binding presumably cause this loss of signal. It is important to note that these experiments probe the kinetics of receptor denaturation rather than the equilibrium distribution. The denaturation was modeled as an irreversible first-order process, and the data were fit using nonlinear regression analysis. The melting temperature (T_M) is defined as the point at which 50% (calculated) of the receptor is unfolded (see Materials and Methods for a description of models

and curve fits). Because the process is kinetically controlled, the apparent T_M is dependent on the time of heat treatment. For further discussion of this subject, please see the Supporting Information.

The thermal stability of CCR5 was measured in the presence and absence of high-affinity small molecule receptor ligands. CCR5 solubilized in buffer N has a T_M of 47.1 ± 0.6 °C (Figure 4A, black). Preincubation of CCR5 with 8 μM maraviroc, AD101, CMPD 167, or vicriviroc before the application of heat conferred a significant increase in thermal stability (Figure 4A,B). Maraviroc stabilizes CCR5 to the greatest extent, shifting the T_M to 66.0 ± 0.3 °C (Figure 4A, red). The T_M values for AD101, CMPD 167, and vicriviroc are 59.9 ± 1.0, 62.7 ± 2.3, and 59.5 ± 1.4 °C, respectively (Figure 4B). Another interesting effect of these ligands is the reduction of the level of 2D7-EuK binding. Preincubation with all ligands results in a decrease in the magnitude of the HTRF signal, but to varying degrees. This indicates that antagonist binding reduces the accessibility of the 2D7 epitope on the EC2 loop, consistent with earlier work (*23*). In addition, each of these melting curves displays an increase in the signal near 50 °C before complete loss due to denaturation. This profile suggests that at least two distinct binding states might be involved in the antagonist−CCR5 interaction, with the "slower" being more amenable to 2D7 binding. These ligand−CCR5 denaturation curves were modeled as a sequence of two irreversible first-order processes. It is interesting that the conversion of the two inhibitor-bound conformations occurs around the temperature at which the empty receptor is denatured. The molecular structures of the antagonists tested are shown in Figure 4C.

Similar measurements were taken for CCR5 NABBs (Figure 4D). There are several notable features of the CCR5 NABB melting curve. The T_M shifts to 54.5 ± 3.4 °C, suggesting that incorporation into the native membranelike environment of NABBs improves the thermal stability of CCR5. Interestingly, the dramatic shift in melting temperature after preincubation with maraviroc is not observed for CCR5 NABBs (data not shown). In addition, the temperature range over which the magnitude of the signal decreases is significantly broadened compared with that of solubilized CCR5, suggesting some sample heterogeneity or a lower activation energy associated with denaturation.

DISCUSSION

CCR5 is an important class A (rhodopsin-like) GPCR because of its role as a primary HIV-1 coreceptor (*24*, *25*). Its natural ligands, including MIP-1α, MIP-1β, and RANTES, are potent inhibitors of HIV infection, and a number of small molecule antagonists that block HIV entry have been reported (*26*, *27*). Detailed molecular studies of purified CCR5 are important for understanding its biological function, role in HIV entry, and mode of binding to pharmacological agents, but its high lability in solution makes it a particularly challenging target. Some progress has been made, as detergent conditions that maintain proper CCR5 folding for several hours have been identified (*22*, *28*). These reports use binding of the well-characterized conformationally sensitive 2D7 mAb as a reporter for receptor folding and integrity (*29*−*31*).

GPCRs are notoriously difficult to stabilize in a purified system. This challenge is amplified when the receptors cannot be expressed at high levels, as with CCR5. We estimate that 1 μg of CCR5 can be obtained from one 10 cm plate of transfected HEK cells, so an extremely sensitive quantitative assay is desirable. Ideally, this assay should also be capable of high throughput so that a large number of potentially stabilizing conditions can be screened in parallel. We decided on a strategy of HTRF, with fluorescently labeled antibodies forming an immunosandwich on distinct epitopes of CCR5. The key reporter is binding of EuK-labeled 2D7 mAb, which binds to the conformationally sensitive split epitope QKEGL-TL on the EC2 loop of the receptor (*32*, *33*).

HTRF occurs when a EuK fluorescent donor is brought into the proximity of a modified allophycocyanin (XL665) acceptor (*34*, *35*). The dual-wavelength detection of donor (615 nm) and acceptor (665 nm) fluorescence after EuK excitation at 320 nm results in a specific signal with excellent well-to-well reproducibility and internal correction for inner filter effects (*34*, *35*). The signal is time-resolved because of the exceptionally long flourescence lifetime of EuK, reducing the contribution from autofluorescence. The EuK-XL665 FRET pair also has an unusually large Förster radius, approximately 95 Å (*34*, *36*), which permits the transfer of resonance energy from the extracellular to intracellular side of the receptor. The 2D7 mAb was directly labeled with EuK to maximize sensitivity. We developed an efficient solid-phase microlabeling strategy for this conjugation, permitting reaction with quantities of antibody and EuK label much smaller than those previously reported (*19*, *20*, *37*). This procedure resulted in high yields and can be generalized to any IgG molecule or His-tagged protein. This method is particularly advantageous when the labels or antibodies are expensive and a small reaction scale is desired. Biotinylated 1D4 mAb, which recognizes the engineered C-terminal epitope TETSQVAPA, binds streptavidin-XL665 (SA-XL665) to complete the immunosandwich. This assay is capable of detecting ~1 fmol of correctly folded CCR5 in a single 384-microtiter plate well.

The assay is also more informative than immunoblots, as it reports on the quality of the receptor as well as the quantity. Unlike surface plasmon resonance (SPR), conditions can be screened without the need for a common binding buffer and the time-consuming microchip regeneration step. If automated, the HTRF approach described herein combines high-throughput capability and sensitivity at a level exceeding even the best available SPR equipment, which is also more expensive (*38*).

The assay capabilities enabled optimization of incorporation of CCR5 into NABBs, and the best procedure results in a >15% overall yield of folded receptor with the majority of the receptor able to bind 2D7. Because the expression, purification, and NABB formation steps can be scaled, adequate quantities of CCR5 NABBs for structural and biochemical studies should be attainable, especially using inducible suspension-adapted stable cell lines or Sf9 insect cells. The defined lipid bilayer of NABBs could be a particularly attractive platform for single-molecule studies of receptor activation, possibly in combination with microfluidics approaches, because GPCR aggregation phenomena endemic to detergents are of less concern (*39*).

Most auspiciously, the HTRF assay permits high-throughput measurements of CCR5 thermal stability with small amounts of material. These experiments are crucial for determining conditions suitable for structural studies. Because CCR5 retained proper folding in the optimal detergent/lipid mixture even after being heated at >40 °C for 30 min, the solubilized receptor might be more stable than previously thought. Preincubation with small molecule CCR5 antagonists resulted in a marked shift of the T_M to 59−66 °C.

The antagonists maraviroc (*40*), AD101 (*41*), CMPD 167 (*42*), and vicriviroc (*43*) block interaction of CCR5 with the HIV envelope glycoprotein gp120 and demonstrate high antiviral potency. Maraviroc, in particular, has proven to be a promising adjuvant anti-HIV drug. Key residues in the transmembrane domains that are required for antagonist binding have been identified, but precisely how gp120 inhibition occurs remains unknown (*44*, *45*). The melting curves generated (Figure 4) demonstrate that ligand−receptor complexes under optimized conditions could be sufficiently stable for high-temperature NMR or crystallization studies. The profiles also shed some light on the binding dynamics of these antagonists, which appear to consist of two steps. The first state, with a decreased HTRF signal, could be due to slightly decreased 2D7-EuK affinity or an alteration of the antibody binding orientation that results in a longer donor−acceptor distance. The second state, characterized by a notable rise, seems to more closely resemble CCR5 in the absence of antagonist. Interestingly, the four antagonists tested inhibit 2D7-EuK binding to varying extents. The fact that maraviroc has the smallest effect on 2D7 binding might prove useful for combination therapy with CCR5-based vaccines or therapeutic anti-CCR5 antibodies.

Incorporation of CCR5 into NABBs also confers improved thermal stability to CCR5. Surprisingly, the lipid composition of the bilayer or preincubation of CCR5 with maraviroc did not significantly change the melting profile (data not shown). In contrast, rhodopsin in NABBs exhibits the high thermal stability of the inverse agonist-bound state in membranes (*8*).

In summary, we report a rapid and highly efficient solid-phase method for labeling IgG with EuK, and we used the labeled IgG to establish an HTRF method for sensitive and high-throughput quantification of CCR5. The extension of the methodology to other GPCRs is limited only by the availability of suitable antibodies. Such mAbs have already been produced for CXCR4 (*46*) and the 5-hydroxytryptamine (5HT) receptor (*47*). The assay enables optimization and characterization of GPCR reconstitution procedures that would otherwise be extremely burdensome or expensive. Thermal stability measurements of CCR5 and other GPCRs under a variety of conditions could greatly facilitate structural studies. We show, for example, that maraviroc, AD101, CMPD 167, and vicriviroc greatly enhance the thermal stability of CCR5 in detergent solution. In addition, these experiments provide some insight into the dynamics of antagonist binding, which could be therapeutically valuable for a highly targeted receptor like CCR5.

ACKNOWLEDGMENT

We thank Pallavi Sachdev, Ana Vitória Botelho, Manija A. Kazmi, and members of the Sakmar laboratory. We also acknowledge the generous support and encouragement of several private foundations and individuals.

SUPPORTING INFORMATION AVAILABLE

FL-maraviroc standard curve used to calibrate the HTRF assay, a flowchart showing the procedure for incorporating CCR5 into NABBs on a microscale, additional discussion of the denaturation model, including the dependence of the apparent T_M on incubation time. This material is available free of charge via the Internet at http://pubs.acs.org.

REFERENCES

1. Deupi, X., and Kobilka, B. (2007) Activation of G Protein Coupled Receptors. In Mechanisms and Pathways of Heterotrimeric G Protein Signaling, pp 137−166, Elsevier Academic Press Inc., San Diego.
2. Premont, R. T., and Gainetdinov, R. R. (2007) Physiological roles of G protein-coupled receptor kinases and arrestins. *Annu. Rev. Physiol. 69*, 511–534.
3. Lagerstrom, M. C., and Schioth, H. B. (2008) Structural diversity of G protein-coupled receptors and significance for drug discovery. *Nat. Rev. Drug Discovery 7*, 339–357.
4. Rosenbaum, D. M., Rasmussen, S. G. F., and Kobilka, B. K. (2009) The structure and function of G-protein-coupled receptors. *Nature 459*, 356–363.
5. Bartfai, T., Benovic, J. L., Bockaert, J., Bond, R. A., Bouvier, M., Christopoulos, A., Civelli, O., Devi, L. A., George, S. R., Inui, A., Kobilka, B., Leurs, R., Neubig, R., Pin, J. P., Quirion, R., Roques, B. P., Sakmar, T. P., Seifert, R., Stenkamp, R. E., and Strange, P. G. (2004) The state of GPCR research in 2004. *Nat. Rev. Drug Discovery 3*, 574–626.
6. Ernst, O. P., Gramse, V., Kolbe, M., Hofmann, K. P., and Heck, M. (2007) Monomeric G protein-coupled receptor rhodopsin in solution activates its G protein transducin at the diffusion limit. *Proc. Natl. Acad. Sci. U.S.A. 104*, 10859–10864.
7. Bayburt, T. H., Grinkova, Y. V., and Sligar, S. G. (2002) Self-assembly of discoidal phospholipid bilayer nanoparticles with membrane scaffold proteins. *Nano Lett. 2*, 853–856.
8. Banerjee, S., Huber, T., and Sakmar, T. P. (2008) Rapid incorporation of functional rhodopsin into nanoscale apolipoprotein bound bilayer (NABB) particles. *J. Mol. Biol. 377*, 1067–1081.
9. Whorton, M. R., Bokoch, M. P., Rasmussen, S. G. F., Huang, B., Zare, R. N., Kobilka, B., and Sunahara, R. K. (2007) A monomeric G protein-coupled receptor isolated in a high-density lipoprotein particle efficiently activates its G protein. *Proc. Natl. Acad. Sci. U.S.A. 104*, 7682–7687.
10. Yoshiura, C., Kofuku, Y., Ueda, T., Mase, Y., Yokogawa, M., Osawa, M., Terashima, Y., Matsushima, K., and Shimada, I. (2010) NMR analyses of the interaction between CCR5 and its ligand using functional reconstitution of CCR5 in lipid bilayers. *J. Am. Chem. Soc. 132*, 6768–6777.
11. Maurel, D., Kniazeff, J., Mathis, G., Trinquet, E., Pin, J. P., and Ansanay, H. (2004) Cell surface detection of membrane protein interaction with homogeneous time-resolved fluorescence resonance energy transfer technology. *Anal. Biochem. 329*, 253–262.
12. Albizu, L., Balestre, M. N., Breton, C., Pin, J. P., Manning, M., Mouillac, B., Barberis, C., and Durroux, T. (2006) Probing the existence of g protein-coupled receptor dimers by positive and negative ligand-dependent cooperative binding. *Mol. Pharmacol. 70*, 1783–1791.
13. Albizu, L., Teppaz, G., Seyer, R., Bazin, H., Ansanay, H., Manning, M., Mouillac, B., and Durroux, T. (2007) Toward efficient drug screening by homogeneous assays based on the development of new fluorescent vasopressin and oxytocin receptor ligands. *J. Med. Chem. 50*, 4976–4985.
14. Serrano-Vega, M. J., Magnani, F., Shibata, Y., and Tate, C. G. (2008) Conformational thermostabilization of the β1-adrenergic receptor in a detergent-resistant form. *Proc. Natl. Acad. Sci. U.S.A. 105*, 877–882.
15. Alexandrov, A. I., Mileni, M., Chien, E. Y. T., Hanson, M. A., and Stevens, R. C. (2008) Microscale fluorescent thermal stability assay for membrane proteins. *Structure 16*, 351–359.
16. Yan, E. C. Y., Kazmi, M. A., Ganim, Z., Hou, J. M., Pan, D. H., Chang, B. S. W., Sakmar, T. P., and Mathies, R. A. (2003) Retinal counterion switch in the photoactivation of the G protein-coupled receptor rhodopsin. *Proc. Natl. Acad. Sci. U.S.A. 100*, 9262–9267.
17. Oprian, D. D., Molday, R. S., Kaufman, R. J., and Khorana, H. G. (1987) Expression of a synthetic bovine rhodopsin gene in monkey kidney cells. *Proc. Natl. Acad. Sci. U.S.A. 84*, 8874–8878.
18. Goding, J. W., and Goding, J. W. (1996) Monoclonal antibodies: Principles and practice: Production and application of monoclonal antibodies in cell biology biochemistry and immunology, 3rd ed., Academic Press, Inc., New York.
19. Cummings, R. T., McGovern, H. M., Zheng, S., Park, Y. W., and Hermes, J. D. (1999) Use of a phosphotyrosine-antibody pair as a general detection method in homogeneous time-resolved fluorescence: Application to human immunodeficiency viral protease. *Anal. Biochem. 269*, 79–93.
20. Kane, S. A., Fleener, C. A., Zhang, Y. S., Davis, L. J., Musselman, A. L., and Huang, P. S. (2000) Development of a binding assay for p53/HDM2 by using homogeneous time-resolved fluorescence. *Anal. Biochem. 278*, 29–38.

21. Lopez-Crapez, E., Malinge, J. M., Gatchitch, F., Casano, L., Langlois, T., Pugniere, M., Roquet, F., Mathis, G., and Bazin, H. (2008) A homogeneous resonance energy transfer-based assay to monitor MutS/DNA interactions. *Anal. Biochem. 383*, 301–306.
22. Navratilova, I., Sodroski, J., and Myszka, D. G. (2005) Solubilization, stabilization, and purification of chemokine receptors using biosensor technology. *Anal. Biochem. 339*, 271–281.
23. Tsamis, F., Gavrilov, S., Kajumo, F., Seibert, C., Kuhmann, S., Ketas, T., Trkola, A., Palani, A., Clader, J. W., Tagat, J. R., McCombie, S., Baroudy, B., Moore, J. P., Sakmar, T. P., and Dragic, T. (2003) Analysis of the mechanism by which the small-molecule CCR5 antagonists SCH-351125 and SCH-350581 inhibit human immunodeficiency virus type 1 entry. *J. Virol. 77*, 5201–5208.
24. Allen, S. J., Crown, S. E., and Handel, T. M. (2007) Chemokine: Receptor structure, interactions, and antagonism. *Annu. Rev. Immunol. 25*, 787–820.
25. Lusso, P. (2006) HIV and the chemokine system: 10 years later. *EMBO J. 25*, 447–456.
26. Kuhmann, S. E., and Hartley, O. (2008) Targeting chemokine receptors in HIV: A status report. *Annu. Rev. Pharmacol. Toxicol. 48*, 425–461.
27. Horuk, R. (2009) OPINION Chemokine receptor antagonists: Overcoming developmental hurdles. *Nat. Rev. Drug Discovery 8*, 23–33.
28. Navratilova, I., Dioszegi, M., and Myszka, D. G. (2006) Analyzing ligand and small molecule binding activity of solubilized GPCRs using biosensor technology. *Anal. Biochem. 355*, 132–139.
29. Wu, L. J., LaRosa, G., Kassam, N., Gordon, C. J., Heath, H., Ruffing, N., Chen, H., Humblias, J., Samson, M., Parmentier, M., Moore, J. P., and Mackay, C. R. (1997) Interaction of chemokine receptor CCR5 with its ligands: Multiple domains for HIV-1 gp120 binding and a single domain for chemokine binding. *J. Exp. Med. 186*, 1373–1381.
30. Farzan, M., Mirzabekov, T., Kolchinsky, P., Wyatt, R., Cayabyab, M., Gerard, N. P., Gerard, C., Sodroski, J., and Choe, H. (1999) Tyrosine sulfation of the amino terminus of CCR5 facilitates HIV-1 entry. *Cell 96*, 667–676.
31. Mirzabekov, T., Bannert, N., Farzan, M., Hofmann, W., Kolchinsky, P., Wu, L. J., Wyatt, R., and Sodroski, J. (1999) Enhanced expression, native purification, and characterization of CCR5, a principal HIV-1 coreceptor. *J. Biol. Chem. 274*, 28745–28750.
32. Lee, B., Sharron, M., Blanpain, C., Doranz, B. J., Vakili, J., Setoh, P., Berg, E., Liu, G., Guy, H. R., Durell, S. R., Parmentier, M., Chang, C. N., Price, K., Tsang, M., and Doms, R. W. (1999) Epitope mapping of CCR5 reveals multiple conformational states and distinct but overlapping structures involved in chemokine and coreceptor function. *J. Biol. Chem. 274*, 9617–9626.
33. Khurana, S., Kennedy, M., King, L. R., and Golding, H. (2005) Identification of a linear peptide recognized by monoclonal antibody 2D7 capable of generating CCR5-specific antibodies with human immunodeficiency virus-neutralizing activity. *J. Virol. 79*, 6791–6800.
34. Mathis, G. (1995) Probing molecular interactions with homogeneous techniques based on rare earth cryptates and fluorescence energy transfer. *Clin. Chem. 41*, 1391–1397.
35. Trinquet, E., Maurin, F., Preaudat, M., and Mathis, G. (2001) Allophycocyanin 1 as a near-infrared fluorescent tracer: Isolation, characterization, chemical modification, and use in a homogeneous fluorescence resonance energy transfer system. *Anal. Biochem. 296*, 232–244.
36. Mathis, G. (1993) Rare earth cryptates and homogeneous fluoroimmunoassays with human sera. *Clin. Chem. 39*, 1953–1959.
37. Lopez, E., Chypre, C., Alpha, B., and Mathis, G. (1993) Europium-(III) trisbipyridine cryptate label for time-resolved fluorescence detection of polymerase chain reaction products fixed on a solid support. *Clin. Chem. 39*, 196–201.
38. Rich, R. L., Miles, A. R., Gale, B. K., and Myszka, D. G. (2009) Detergent screening of a G-protein-coupled receptor using serial and array biosensor technologies. *Anal. Biochem. 386*, 98–104.
39. Jastrzebska, B., Maeda, T., Zhu, L., Fotiadis, D., Filipek, S., Engel, A., Stenkamp, R. E., and Palczewski, K. (2004) Functional characterization of rhodopsin monomers and dimers in detergents. *J. Biol. Chem. 279*, 54663–54675.
40. Dorr, P., Westby, M., Dobbs, S., Griffin, P., Irvine, B., Macartney, M., Mori, J., Rickett, G., Smith-Burchnell, C., Napier, C., Webster, R., Armour, D., Price, D., Stammen, B., Wood, A., and Perros, M. (2005) Maraviroc (UK-427,857), a potent, orally bioavailable, and selective small-molecule inhibitor of chemokine receptor CCR5 with broad-spectrum anti-human immunodeficiency virus type 1 activity. *Antimicrob. Agents Chemother. 49*, 4721–4732.
41. Trkola, A., Kuhmann, S. E., Strizki, J. M., Maxwell, E., Ketas, T., Morgan, T., Pugach, P., Xu, S., Wojcik, L., Tagat, J., Palani, A., Shapiro, S., Clader, J. W., McCombie, S., Reyes, G. R., Baroudy, B. M., and Moore, J. P. (2002) HIV-1 escape from a small molecule, CCR5-specific entry inhibitor does not involve CXCR4 use. *Proc. Natl. Acad. Sci. U.S.A. 99*, 395–400.
42. Veazey, R. S., Klasse, P. J., Ketas, T. J., Reeves, J. D., Piatak, M., Kunstman, K., Kuhmann, S. E., Marx, P. A., Lifson, J. D., Dufour, J., Mefford, M., Pandrea, I., Wolinsky, S. M., Doms, R. W., DeMartino, J. A., Siciliano, S. J., Lyons, K., Springer, M. S., and Moore, J. P. (2003) Use of a small molecule CCR5 inhibitor in macaques to treat simian immunodeficiency virus infection or prevent simian-human immunodeficiency virus infection. *J. Exp. Med. 198*, 1551–1562.
43. Strizki, J. M., Tremblay, C., Xu, S., Wojcik, L., Wagner, N., Gonsiorek, W., Hipkin, R. W., Chou, C. C., Pugliese-Sivo, C., Xiao, Y. S., Tagat, J. R., Cox, K., Priestley, T., Sorota, S., Huang, W., Hirsch, M., Reyes, G. R., and Baroudy, B. M. (2005) Discovery and characterization of vicriviroc (SCH 417690), a CCR5 antagonist with potent activity against human immunodeficiency virus type 1. *Antimicrob. Agents Chemother. 49*, 4911–4919.
44. Seibert, C., Ying, W., Gavrilov, S., Tsamis, F., Kuhmann, S. E., Palani, A., Tagat, J. R., Clader, J. W., McCombie, S. W., Baroudy, B. M., Smith, S. O., Dragic, T., Moore, J. P., and Sakmar, T. P. (2006) Interaction of small molecule inhibitors of HIV-1 entry with CCR5. *Virology 349*, 41–54.
45. Kondru, R., Zhang, J., Ji, C., Mirzadegan, T., Rotstein, D., Sankuratri, S., and Dioszegi, M. (2008) Molecular interactions of CCR5 with major classes of small-molecule anti-HIV CCR5 antagonists. *Mol. Pharmacol. 73*, 789–800.
46. McKnight, A., Wilkinson, D., Simmons, G., Talbot, S., Picard, L., Ahuja, M., Marsh, M., Hoxie, J. A., and Clapham, P. R. (1997) Inhibition of human immunodeficiency virus fusion by a monoclonal antibody to a coreceptor (CXCR4) is both cell type and virus strain dependent. *J. Virol. 71*, 1692–1696.
47. Mancia, F., Brenner-Morton, S., Siegel, R., Assur, Z., Sun, Y., Schieren, I., Mendelsohn, M., Axel, R., and Hendrickson, W. A. (2007) Production and characterization of monoclonal antibodies sensitive to conformation in the 5HT2c serotonin receptor. *Proc. Natl. Acad. Sci. U.S.A. 104*, 4303–4308.